Spin alignment based rubidium magnetometry with free spin precession

Yang Li,[1] Lulu Zhang,[1] Yongbiao Yang,[1] Junye Zhao,[1] Yanhua Wang,[2,3] Baodong Yang,[2,3] and Junmin Wang[1,3]
[1)] *State Key Laboratory of Quantum Optics and Quantum Optics Devices, and Institute of Opto-Electronics, Shanxi University, Taiyuan 030006, China*
[2)] *School of Physics and Electronic Engineering, Shanxi University, Taiyuan 030006, China*
[3)] *Collaborative Innovation Center of Extreme Optics, Shanxi University, Taiyuan 030006, China*

(*Electronic mail: wwjjmm@sxu.edu.cn)

(Dated: 11 October 2024)

The optically pumped atomic magnetometry is currently one of the most sensitive instruments for measuring weak magnetic fields. Spin alignment based rubidium magnetometry with free spin precession is implemented experimentally. The 795 nm linearly-polarized pump laser beam (which also serves as probe beam) with the polarization direction along the Y axis is propagated along the Z axis through a cylinder Rb-87 enriched atomic vapor cell with parraffin coating on the inner wall. The Rb atomic vapor cell is positioned inside a cylinder four-layer permalloy magnetic shielding barrel with a typical shielding factor of better than 10000. Meanwhile, three pairs of Helmholtz magnetic coils with low-noise DC or AC currents along the X, Y and Z axises provide the DC magnetic field B_0 along the Y axis and the $\pi/2$ radio-frequency (RF) magnetic field pulse B_{RF} along the Z axis. In this magnetometry, we optimize the parameters of the pump power and RF magnetic field strength. Under the optimized conditions, the sensitivity of spin alignment based rubidium magnetometry with free spin precession is characterized and it is 1.7 pT/Hz$^{1/2}$. Due to the high sensitivity of this magnetometry, it can be an optimal choice for measuring ambient magnetic fields.

I. INTRODUCTION

As an important feature of magnetic objects, magnetic field is one of the earliest physical phenomena recognized by human being, and the precision measurement of magnetic field is also an important physical means for us to understand the world. With the development of science and technology, high-sensitivity magnetic field measurement technology has also been greatly developed. Atomic magnetometry based on quantum theory also come into being. With the continuous development of laser technology, the sensitivity of atomic magnetometry is also improving. It started with 1 nT and grew to 0.1 fT. At present, the types of high-sensitivity magnetometry mainly include nuclear precession magnetometry, optical pump atomic magnetometry[1.2] and superconducting quantum interference magnetometry [3] . Due to its high sensitivity, fast response and wide measurement range, the superconducting quantum interference magnetometry is widely used in the fields of brain magnetic measurement, nuclear magnetic resonance and non-destructive testing[4]. However, due to its huge temperature control equipment, the application range of the superconducting quantum interference magnetometry has great limitations.

The optically pumped atomic magnetometry has been greatly developed due to its advantages of miniaturization and high sensitivity. According to the different polarization of the pump beam, the optical pump magnetometry can be divided into spin-orientation magnetometry and spin-alignment magnetometry. In 2007, Budker's research group proposed a spin alignment optical pump atom magnetometry based on nonlinear magneto-optical rotation effect, which means nonlinear magneto optical rotation magnetometry (NMOR magnetometry)[5]. The atom is polarized by a linearly polarized beam, and a static magnetic field is added to the polarization direction of the polarized beam and a small amplitude alternating magnetic field is added to the beam propagation direction to detect the alternating magnetic field. The calibrated sensitivity of the magnetometry is 10 fT/Hz$^{1/2}$. In 2024, Sheng Zou's research group improved the above magnetometry, changing the small amplitude alternating magnetic field to $\pi/2$ pulse RF magnetic field [6], and adding the repump beam, then detecting the free spin precession decay signal to detect the static magnetic field. Finally, the sensitivity is 0.16 pT/Hz$^{1/2}$ under zero magnetic field and 0.75 pT/Hz$^{1/2}$ under simulated geomagnetic field. In order to improve the practicability and simplicity of optical pump atomic magnetometry, a single beam based optical pump atomic magnetometry is proposed in this paper. Compared with commercially available fluxgate magnetometry in the market, this magnetometry has a higher sensitivity and is therefore of good application value.

In this paper, we design a spin alignment based rubidium magnetometry with free spin precession using linearly polarized beam and $\pi/2$ pulse RF magnetic field. The parameters of the pump beam intensity and the RF magnetic field strength in the magnetometry system are optimized by observing the magnetic resonance signal of the magnetometry, and then the sensitivity of the magnetometry is calculated. The magnetometer uses a single beam design, the linear polarization plane is rotation by the circular dichroism of the light. It works on the same principle as the NMOR magnetometry. Due to the high sensitivity of the magnetometry, it can be an optimal choice for measuring ambient magnetic fields.

II. THEORETICAL ANALYSIS

The physical principle of optically pumped atomic magnetometry is based on the interaction of atomic ensemble with magnetic fields and light fields. It reflects the magnitude of the measured magnetic field by measuring the Larmor precession

frequency of the atomic spin polarization vector in the external magnetic field [7].Alkali metal atoms are commonly used as the medium of interaction with the light field in optically pumped atomic magnetometers, such as rubidium, cesium and so on. As atoms absorb the photons, the ground state atoms transition to the excited state, and the atoms fall back to the ground state due to spontaneous decay. With the continuous pump of photons, the state of atoms will again transition to the excited state, and finally spontaneously decay to the ground state that does not interact with the photon (that is the dark state), completing the optical pump process[8]. When an RF magnetic field is applied, a magnetic dipole transition occurs between adjacent Zeeman energy levels. When the frequency of the RF magnetic field is equal to the precession frequency of the atomic magnetic moment around the magnetic field, that is the Larmor precession frequency, the magnetic dipole transition rate is the largest. However, different types of optically pumped atomic magnetometry have different detection methods for the dynamic evolution behavior of the atomic[9]. For example, the Mz type optically pumped atomic magnetometry uses the magnetic dipole transition caused by the alternating magnetic field to depolarize the atomic ensemble, and then the transmitted beam intensity weakened due to the reabsorption of the beam by the atoms to measure the magnetic field[10] . The spin alignment based rubidium magnetometry with free spin precession takes advantage of the circular dichroism of the light to measure the magnetic field. The circular dichroism of the light is when π polarized beam passes through the vapor cell, the beam polarization rotates due to the different absorption rates of atoms for σ^+ polarized beam and σ^+ polarized beam components[11]. The measurement principle is the same as that of the NMOR magnetometry.

A. Preparation of spin alignment of Rb-87 atoms

The first step in measuring a magnetic field with an optically pumped atomic magnetometry is to polarize the atom. The atomic polarization state is defined as: if the atoms in an ensemble are all in the same quantum state, then the entire ensemble can be described by a wave function, and the atoms are in a polarized state. In magnetometry system, optical pump technology is used to realize the polarization of the atomic ensemble. The different polarization states of the pumped beam will polarize the atomic ensemble into different polarization states. The 795 nm linearly polarized pump beam resonating to the D1 line (F_g=2) - (F_e=1) of the Rb-87 atom excites the atom from the ground state to the excited state, and then the excited atom returns to the various Zeeman levels of the ground state by spontaneous decay. With the continuous excitation of linearly polarized pumped beam, most of the atoms finally lie on the m_F=-2 and m_F=+2 of the ground state. At this time, there are still some atoms in other Zeeman levels in the ground state, completing the preparation of the spin alignment of Rb-87 atoms. The Figure 1. shows the physical image of the spin alignment based rubidium magnetometry with free spin precession.

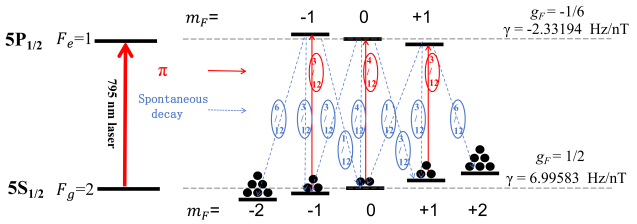

FIG. 1. Atomic spin alignment of Rb-87 atoms prepared by 795 nm linearly polarized laser beam.

B. Simplified atomic spin evolution model

Model construction for transitions of ground state angular momentum $F_g > 1$ is complex. Therefore, for simplicity, a reduced model of the (F_g=1) - (F_e=0) transition is considered to obtain the analytical solution. We describe the density matrix form analysis in the experimental process. The time evolution of the density matrix $\hat{\rho}$ is given by the Liouville equation

$$\frac{d\hat{\rho}}{dt} = -i[\hat{H},\hat{\rho}] - \frac{1}{2}\{\hat{\xi},\hat{\rho}\} + \hat{\Lambda} \tag{1}$$

Where $\hat{H}$ is the total Hamiltonian of the system, $\hat{\xi}$ is the relaxation operator, and $\hat{\Lambda}$ is the repopulation operator

$$\hat{H} = \begin{pmatrix} \Omega_L & \frac{\Omega_{RF}\cos(\omega_{RF}t)}{\sqrt{2}} & 0 & 0 \\ \frac{\Omega_{RF}\cos(\omega_{RF}t)}{\sqrt{2}} & 0 & \frac{\Omega_{RF}\cos(\omega_{RF}t)}{\sqrt{2}} & -\frac{\Omega_R\cos(\omega t)}{\sqrt{3}} \\ 0 & \frac{\Omega_{RF}\cos(\omega_{RF}t)}{\sqrt{2}} & -\Omega_L & 0 \\ 0 & -\frac{\Omega_R\cos(\omega t)}{\sqrt{3}} & 0 & \omega_0 \end{pmatrix} \tag{2}$$

Where, $\Omega_L = \gamma B_0$ is the Larmor precession frequency corresponding to the static magnetic field B_0, where γ is the gyromagnetic ratio of the F_g=1. $\Omega_{RF} = g_F\mu_B B_{RF}/\hbar$ is the magnetic Rabi frequency corresponding to the RF magnetic field B_{RF}, where g_F is the Lande factor of the F_g=1 and μ_B is the Bohr magneton. Ω_R is the Rabi frequency for the optical transition caused by the probe beam, ω is the frequency of the probe beam, ω_{RF} is the frequency of the RF magnetic field and ω_0 is the frequency resonating on the (F_g=1) - (F_e=0). For the case where the RF magnetic field is turned off during detection, the Hamiltonian of the system can be simplified as

$$\hat{H}' = \begin{pmatrix} \Omega_L & 0 & 0 & 0 \\ 0 & 0 & 0 & -\frac{\Omega_R}{2\sqrt{3}} \\ 0 & 0 & -\Omega_L & 0 \\ 0 & -\frac{\Omega_R}{2\sqrt{3}} & 0 & 0 \end{pmatrix}. \tag{3}$$

The relaxation rate of the system can be given by the following matrix

$$\hat{\xi} = \begin{pmatrix} \gamma & 0 & 0 & 0 \\ 0 & \gamma & 0 & 0 \\ 0 & 0 & \gamma & 0 \\ 0 & 0 & 0 & \Gamma+\gamma \end{pmatrix} \tag{4}$$

Where, γ is the uniform relaxation rate of the ground state and excited state, and its related factors include the wall collisions, buffer gas collisions, diffusion of atoms from the beam beam area, or unpolarized atoms flow from the vapor cell stem. Γ is the relaxation rate of the excited state, mainly due to the spontaneous decay of the excited state atoms. The matrix $\hat{\Lambda}$ describes the repopulation of the number of atoms in the ground state due to the spontaneous decay of atoms in the excited state, and is represented by the following matrix:

$$\hat{\Lambda} = \begin{pmatrix} \frac{\gamma+\Gamma\rho_{e_0e_0}}{3} & 0 & 0 & 0 \\ 0 & \frac{\gamma+\Gamma\rho_{e_0e_0}}{3} & 0 & 0 \\ 0 & 0 & \frac{\gamma+\Gamma\rho_{e_0e_0}}{3} & 0 \\ 0 & 0 & 0 & 0 \end{pmatrix} \tag{5}$$

The time evolution of the elements in the density matrix is determined by the Liouville equation. As shown below:

$$\frac{d\rho_{g_{\pm1}e_0}}{dt} = -\left(\frac{\Gamma}{2}+\gamma\pm i\Omega_L\right)\rho_{g_{\pm1}e_0} - \frac{i\Omega_R\rho_{g_{\pm1}g_0}}{2\sqrt{3}} \tag{6}$$

$$\frac{d\rho_{g_{\pm1}g_0}}{dt} = -\frac{i\Omega_R\rho_{g_{\pm}e_0}}{2\sqrt{3}} - (\gamma\pm i\Omega_L)\rho_{g_{\pm1}g_0} \tag{7}$$

The subscript of $\rho_{g_{\pm1}e_0}$ in the above formula represents the Zeeman sub-level, which can be expressed as the particle population change caused by the relaxation rate of the excited state is significantly greater than that caused by other factors, $\rho_{g_{\pm1}e_0}$ can be represented by the equation(8), where a and b are real numbers:

$$\rho_{g_{\pm1}e_0} = \frac{(-ai+b)e^{t(-\gamma\mp i\Omega_L)}\Omega_R}{\sqrt{3}\Gamma} \tag{8}$$

From the expectation value of the polarization of the medium, the optical-rotation signal per unit length dl of the medium can be written in the form of equation(9)[12].

$$\frac{d\theta}{dt} = \frac{\sqrt{3}n_d\Gamma\lambda^2}{2\sqrt{2}\pi\Omega_R}\,\mathrm{Im}\left(\rho_{g_{-1}e_0}-\rho_{g_1e_0}\right) \tag{9}$$

Which λ refers to the wavelength of probe beam, n_d is the atomic density. Combined with the above equation, the magnitude of the optical rotation signal can be expressed as

$$\frac{d\theta}{dt} = \frac{bn_d\lambda^2}{2\sqrt{2}\pi}e^{-t\gamma_{\gamma f}}\sin(\Omega_L t) \tag{10}$$

Equation (10) shows that the signal is an exponentially decayed sine wave whose frequency corresponds to the Larmor precession frequency.

III. EXPERIMENTAL SETUP

As shown in the Figure 2. the spin alignment based rubidium magnetometry with free spin precession is implemented experimentally. The experiment utilizes a cylinder Rb-87 enriched atomic vapor cell with parraffin coating on the inner wall. The Rb atomic vapor cell has a diameter of 25 mm and a length of 75 mm. The Rb atomic vapor cell is positioned inside a cylinder four-layer permalloy magnetic shielding barrel with a typical shielding factor of better than 10000. The 795 nm linearly-polarized pump laser beam (which also serves as probe beam) with the polarization direction along the Y axis is propagated along the Z axis through the Rb atomic vapor cell at room temperature. The pump beam with a waist radius of about 10 mm is tuned on Rb-87 D_1 line F_g=2→F_e=1 transition by the polarization spectroscopic device. Meanwhile, three pairs of Helmholtz magnetic coils with low-noise DC or AC currents along the X, Y and Z axises provide the DC magnetic field B_0 along the Y axis and the $\pi/2$ RF magnetic field pulse B_{RF} along the Z axis. The frequency of the RF magnetic field resonates with the Larmor precession frequency. The balanced differencial photodiodes data is obtained by data acquisition card (NI USB-6363), which is the free spin precession decay signal. Then the magnetic resonance signal is obtained by the fast Fourier transform.

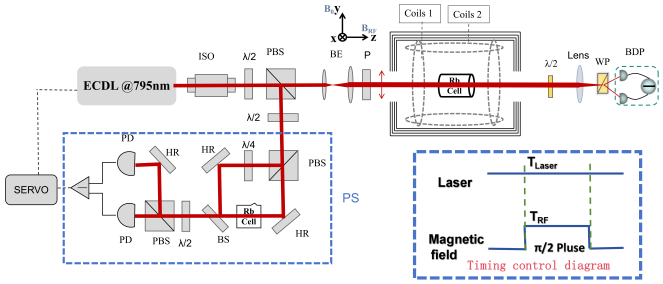

FIG. 2. The schemetic diagram of experimental setup of the spin alignment based rubidium magnetometry with free spin precession. ECDL: external-cavity diode laser; ISO: optical isolator; $\lambda/2$:half-wave plate; PBS: polarization beam splitter; BE:the beam expanding telescope; P: polarizer; Coils 1,Coils 2: Helmholtz coils; WP: Wollaston prism; BDP: balanced differencial photodiodes; $\lambda/4$:quarter-wave plate; HR: high-reflectivity mirror; BS: beam splitter mirror; PD: photodetector; PS: the polarization spectroscopic device.

The frequency of the RF magnetic field is kept in resonance with the Larmor precession frequency and the RF magnetic field is controlled periodically. At the initial moment, the linearly polarized beam passing through the atomic vapor cell to polarized atoms. $\pi/2$ RF magnetic resonance pulse make the atomic magnetic moment gradually precess to the RF magnetic field direction. $\pi/2$ RF magnetic resonance pulse duration can be calculated by the equation (11).

$$t_{\pi/2} = \frac{\pi}{2\Omega_{RF}} \tag{11}$$

After the RF magnetic field is turned off, the atom will be re-polarized, and the atomic magnetic moment will precess around the direction of the static magnetic field. Due to the circular dichroism of the light, when π polarized beam passes through the atomic vapor cell, the σ^+ polarized beam and the

σ^- polarized beam components of the π polarized beam are absorbed differently by the vapor cell, resulting that the polarization plane of the light field rotates. At this time, the free spin precession decay signal can be detected by the balanced differential detector. By fast Fourier transform the time-domain signal to the frequency-domain signal and the Larmor precessional frequency can be extracted through Lorentz line fitting [13.14].

IV. EXPERIMENTAL RESULTS AND DISCUSSIONS

Spin alignment based rubidium magnetometry with free spin precession is implemented experimentally to perform periodic control on the RF magnetic field. In a period, when the RF magnetic field is turned off, the free spin precession signal is transformed by the fast Fourier transform to obtain the magnetic resonance signal. The Larmor precession frequency is extracted after Lorentz line fitting of the magnetic resonance signal. The transverse relaxation time T_2 of atomic ensemble is obtained by fitting the free spin precession decay signal. The Figure 3. and Figure 4. are a magnetometry signal diagram and a magnetic resonance signal diagram.

According to the deduction of equation (10), the decaying signal of free spin precession in Figure 3. is an exponential decaying positive wave with a frequency of Larmor precession, while the magnetic resonance signal in Figure 4. shows that the resonance frequency is Larmor precession frequency, which conforms to the theoretical expectation. The relationship between T_2 and HWHM of magnetic resonance signal is

$$T_2 \sim \frac{1}{\Delta\upsilon} \tag{12}$$

In the equation(12), T_2 represents the transverse relaxation time, $\Delta\upsilon$ representing the HWHM of magnetic resonance signal, T_2 is inversely proportional to $\Delta\upsilon$.

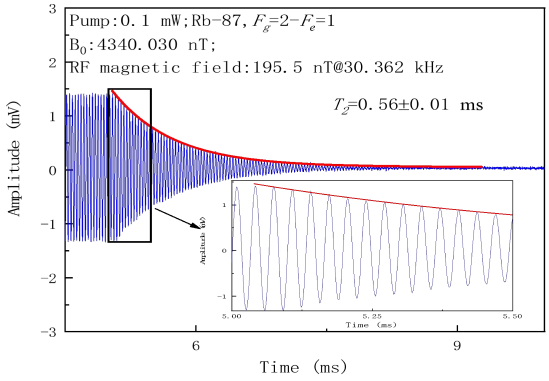

FIG. 3. Typical free spin procession signal of the spin alignment based rubidium-87 magnetometry after the $\pi/2$ radio-frequency magnetic field pulse.Spin transverse relaxation time of rubidium-87 spin alignment state, T_2, is about 0.56 ms obtained by exponential decay fitting. The inset is a zooming view of the partial signal of free spin procession.

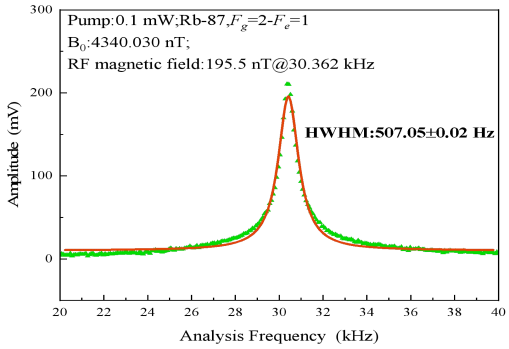

FIG. 4. The magnetic resonance signal is achieved by FFT of the free spin procession signal of the rubidium-87 spin alignment (the green dots).The red curve is Lorentzian fitting. Typical half-width half-maximum (HWHM) linewidth of the magnetic resonance signal is about 507.05 Hz.

A. Parameter optimization

After the magnetic resonance signal is obtained, the RF magnetic field strength and the polarized beam intensity in the magnetometry system are changed. The amplitude of the magnetic resonance signal, the HWHM and slope (that is the ratio of the amplitude of the magnetic resonance signal to the HWHM of the magnetic resonance signal) are observed as the variable changed.

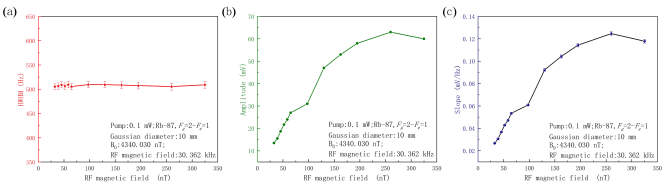

FIG. 5. (a) HWHM VS RF magnetic field strength (b) Amplitude VS RF magnetic field strength (c) Slope VS RF magnetic field strength

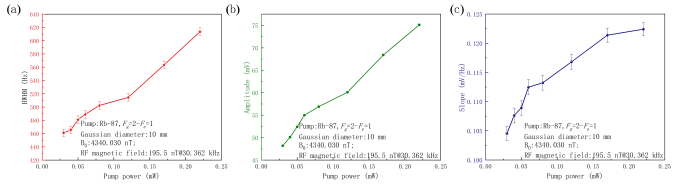

FIG. 6. (a) HWHM VS Pump power (b) Amplitude VS Pump power (c) Slope VS Pump power

Figure 5. and Figure 6. respectively show the changes of the amplitude, HWHM and slope of the magnetic resonance signal with the change of the RF magnetic field and the change of the pump power. Figure 5. (a) shows that the HWHM of the magnetic resonance signal do not change greatly with the change of the RF magnetic field because the RF magnetic field has been turned off when the free spin precession decay signal is obtained. Figure 5. (b) and Figure 5. (c) show

that the magnetic dipole transition rate increases within a certain range with the increase of the RF magnetic field strength, and then reaches saturation. Therefore, with the increase of the RF magnetic field strength, the amplitude and slope of the magnetic resonance signal increase within a certain range, and then tend to be stable. Figure 6. (a), Figure 6. (b) and Figure 6. (c) show that as the polarized beam intensity increases within a certain range, the optical pump rate gradually increases, so the HWHM, signal amplitude and slope of the magnetic resonance signal gradually increase. Because the magnetometry sensitivity is related to the narrow line width and amplitude of the magnetic resonance signal, the magnetometry sensitivity is calculated by selecting the appropriate parameters in the figure above.

B. Experimental results

According to the amplitude and HWHM of the processed magnetic resonance signal, the strength of the RF magnetic field is set to 195.5 nT and the pumped power of the pump beam is 0.1mW. After that, the spin alignment based rubidium magnetometry with free spin precession signals of multiple periods are recorded through LabVIEW program. A power spectrum density (PSD) program is written in Matlab language to calculate the static magnetic field B_0 and magnetometry sensitivity, and to calibrate the sensitivity and the static magnetic field B_0 of the magnetometry by statistical average.

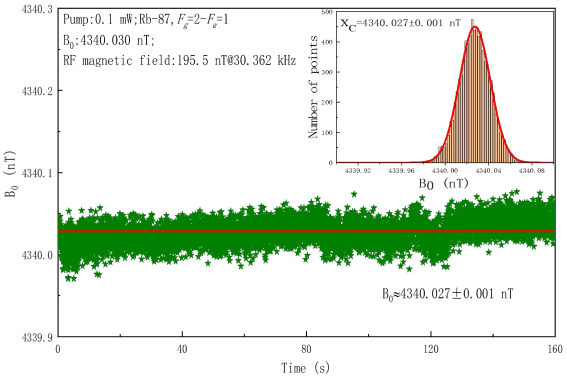

FIG. 7. The 4000 green asterisk dots represent the static magnetic field values. Each value is calculated from a free spin precession signal with a period of 20 milliseconds. The red line indicates the static magnetic field value after statistical average. Typical static magnetic field value is about 4340.027 nT. The inset shows the typical static magnetic field values obtained after statistical average and Gaussian fitting of the static magnetic field values for 4000 periods.

Through Gaussian fitting of the frequency statistical distribution in Figure 7., statistical average is carried out, and the calculated magnetic field B_0 value is 4340.030 nT. Figure 8. shows the noise PSD at the analysis frequency of 0-25 Hz. Since the noise at 0-1 Hz is relatively large and does not meet the statistical standard, the frequency distribution statistics and Gaussian fitting of the noise PSD at the analysis frequency of 1-25 Hz are carried out. The sensitivity of spin alignment based rubidium magnetometry with free spin precession is 1.7 pT/Hz$^{1/2}$.

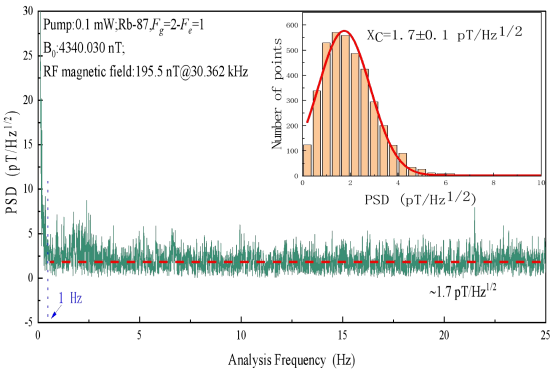

FIG. 8. The green curve shows the PSD calculated from 4000 static magnetic field values, and the red dashed line shows the magnetometry sensitivity obtained from the statistical average of the analysis frequency 1-25Hz of the PSD. Typical magnetometry sensitivity is about 1.7 pT/Hz$^{1/2}$. The inset shows the magnetometry sensitivity obtained after statistical average and Gaussian fitting of the analysis frequency 1-25Hz of the PSD.

V. CONCLUSIONS

In conclusion, spin alignment based rubidium-87 atomic magnetometer with free spin procession is implemented and characterized experimentally by using of single 795 nm linearly polarized laser beam, which serves as the pump beam and the probe beam, passing through a paraffin-coated rubidium-87 enriched vapor cell.The rubidium vapor cell as the sensor element is positioned in a four-layer permally cylindrical magnetic shield with typical shielding factor of better than 10000. The $\pi/2$ RF magnetic field pulse is applied to the spin alignment state of rubidium-87 atoms. The pump power and RF magnetic field strength in the magnetometry system are optimized, and the sensitivity of spin alignment based rubidium magnetometry with free spin precession is 1.7 pT/Hz$^{1/2}$.

In the subsequent experiments, the line width of the magnetic resonance signal can be narrowed by improving the beam diameter of the polarized beam or the magnetic field uniformity at the position of the atomic vapor cell. The polarized beam intensity noise in the magnetometry system and the current noise of the magnetic field current source can also be optimized.

Compared with the absorption-based scheme, linearly polarized detection beam and balanced detection greatly reduce the influence of common-mode noise and laser intensity fluctuations on the magnetometry sensitivity. This magnetometry devoid of heating structures, can be easily fabricated and represents an optimal choice for measuring ambient magnetic fields. The single beam design and high sensitivity of this magnetometry have certain significance for simplifying the commercial optical pump atomic magnetometry.

VI. ACKNOWLEDGEMENTS

This work is supported by the National Natural Science Foundation of China (Grant No.12474483) and Fundamental Research Program of Shanxi Province of China (Grant No.202403021211013)

[1]D. Budker and M. Romalis© "Optical magnetometry," Nature Physics **3**, 227 (2007).
[2]W. M. Sun, J. H. Zhang and X. J. Zeng© "Principle and application of optical atomic magnetometry," (Science Press, 2022). (in Chinese)
[3]J. Clarke, "Principles and applications of SQUIDs," Proceedings of the IEEE **77**, 1208 (1989).
[4]S. H. Ward and K. A. Ruddock, "A field experiment with a rubidium-vapor magnetometry," Journal of Geophysical Research **67**, 1889 (1962).
[5]M. P. Ledbetter, V. M. Acosta, S. M. Rochester, D. Budker, S. Pustelny and V. V. Yashchuk, "Detection of radio-frequency magnetic fields using nonlinear magneto-optical rotation," Physical Review A **75**, 023405 (2007).
[6]G. Jin, T. Shi, Y. Zhao, H. Zhang and S. Zou, "A room-temperature operational alignment magnetometry utilizing free-spin precession," Advanced Quantum Technologies **7**, 2300377 (2024).
[7]H. Haken and H. C. Wolf, "The physics of atoms and quanta : Introduction to experiments and theory," (Springer Science, 2006).
[8]M. Auzinsh, D. Budker and S. Rochester, " Optically polarized atoms," (Oxford University Press, 2010).
[9]F. Bloch, "Nuclear induction," Physical Review **70**, 460 (1946).
[10]L. L. Zhang, L. L. Bai, Y. L. Yang, Y. B. Yang, Y. H. Wang, X. Wen, J. He and J. M. Wang, "Improving the sensitivity of optically pumped Rubidium atom magnetometry with inverse pumping light," Acta Physica Sinica **70**, 230702 (2021). (in Chinese)
[11]R. Jimnez-Martnez, W. C. Griffith, S. Knappe, J. Kitching and M. Prouty, "High-bandwidth optical magnetometry," Journal of the Optical Society of America B **29**, 3398 (2012).
[12]T. Zigdon, A. D. Wilson-Gordon, S. Guttikonda, E. J. Bahr, O. Neitzke, S. M. Rochester and D. Budker, "Nonlinear magneto-optical rotation in the presence of a radio-frequency field," Optics Express **18**, 25494 (2010).
[13]L. M. Rushton, L. Elson, A. Meraki and K. Jensen, "Alignment-based optically pumped magnetometry using a buffer-gas cell," Physical Review Applied **19**, 064047 (2023).
[14]D. Budker, D. F. Kimball, S. M. Rochester and V. V. Yashchuk, "Nonlinear magneto-optical rotation via alignment-to-orientation conversion," Physical Review Letters **85**, 2088 (2000).